Line ratios for soft-x-ray emission following charge exchange between O^{8+} and Kr

D. G. Seely, V. M. Andrianarijaona, D. Wulf, K. Morgan, D. McCammon, M. Fogle, P. C. Stancil, R. T. Zhang, and C. C. Havener

Phys. Rev. A **95**, 052704 — Published 15 May 2017

DOI: 10.1103/PhysRevA.95.052704

Line ratios for soft X-ray emission following charge exchange between O^{8+} and Kr

D. G. Seely*

Department of Physics, Albion College, Albion, Michigan 49224, USA

V. M. Andrianarijaona

Department of Physics, Pacific Union College, Angwin, California 94508, USA

D. Wulf, K. Morgan, and D. McCammon

Department of Physics, University of Wisconsin, Madison, Wisconsin 53706, USA

M. Fogle

Department of Physics, Auburn University, Auburn, Alabama 36849, USA

P. C. Stancil

Department of Physics and Astronomy and the Center for Simulational Physics, University of Georgia, Athens, Georgia 30602-2451, USA

R. T. Zhang and C. C. Havener

Oak Ridge National Laboratory, Oak Ridge, Tennessee 37831, USA

(Dated: April 12, 2017)

Abstract

Lyman spectra and line ratios are reported for soft X-ray emissions following the charge exchange process in 293 km/s, 414 km/s, 586 km/s, and 1256 km/s O^{8+} and Kr collisions. Lyman series from Ly-α to Ly-ε were resolved for the O^{7+} ion using a high resolution X-ray quantum microcalorimeter detector. It is found that the observed line ratios are dependent on the nl distribution of the captured electron, and the Ly-α and Ly-β X-ray emissions are enhanced. Moreover, by comparing the measured line ratios to the constructed theoretical single charge exchange line ratios for O^{8+} + H, it is suggested that autoionizing double capture plays a significant role in the enhancement of Ly-α and Ly-β emissions for the present system.

PACS numbers: 34.70.+e 34.50.-s

* dseely@albion.edu

I. INTRODUCTION

Charge exchange (CX) between highly charged ions and neutral atoms or molecules is a process where one or more target electrons are transferred onto the ion. In particular, low energy CX is important due to its large cross section ($\sim q \times 10^{-15}$ cm^2, q is projectile charge state), and the subsequent X-ray emission can provide details about the astrophysical plasma environment[1–3]. For example, solar wind charge exchange (SWCX) X-ray emission is well understood as the result of CX between solar-wind ions (C^{6+}, N^{7+}, O^{8+}, etc.) and interplanetary neutrals (H, He, etc.)[4, 5]. Cravens [6] developed an analytic model that predicted 25% - 50% of the soft X-ray background could come from SWCX. It has also been suggested that part of the soft-X-ray background below 1 keV photon energy is due to CX between the solar wind and neutrals either in the geocorona or in the heliosphere [6, 7]. This is supported by observations [7, 8]. Recently, Koutroumpa *et al.* [9] have extended the SWCX model and concluded that CX could contribute to nearly all the X-ray flux in some directions. However, these models have suffered from a lack of ion-atom CX data.

Various theoretical models [10] were developed for low energy CX processes where the collision velocity is smaller than the orbital velocity of the active target electron [11]. These include the classical trajectory Monte Carlo (CTMC), atomic orbital close coupling (AOCC) and semi-classical molecular orbital close-coupling (MOCC) methods along with the more recent two-center basis generator method (TC-BGM) . Atomic orbital close coupling (AOCC) approaches work well for calculating total cross sections of CX involving light ions [12, 13]. At very low energies (e.g., the collision energy ≤ 100 eV/u), straight line or classical trajectories are not suitable, therefore the quantum molecular orbital close coupling (QMOCC) methods are more appropriate. Other simpler approaches include the velocity-independent approximations like the classical over-the-barrier model (CBM) [14, 15] which has had some success in predicting the principal quantum number n and the average value of the angular momentum quantum number l for the captured electron. However, predicting state selective cross sections for the CX process remains a theoretical challenge.

X-ray spectra resulting from the process of CX between highly charged ions and atoms are very sensitive to the (n, l) state of the capture electron. X-ray spectra and line ratios measurements can be used to test our understanding of CX collision mechanisms. For example, our previous line ratio measurements [16, 17] for C^{6+} on He and H_2 collisions have

been compared to recent theoretical line ratios constructed from calculations using the TC-BGM method. The satisfactory agreement with our line ratio measurements confirm the predictions that a statistical l distribution occurs at low velocities, while the l distribution shifts to maximum l at high velocities [10]. For C^{6+} on Kr collisions, a true double capture was found to be insignificant [18].

CX with atomic hydrogen, because of its importance in many astrophysical contexts and its simplicity, is often used as a model system for CX in solar wind environments. This model system has been studied by Shipsey *et al.* [19] using MOCC, Fritsch *et al.* [20] using AOCC, and Richter *et al.* [21] using so-called hidden crossing theory with adiabatic molecular states (advanced adiabatic approach) (HCT-AAA). Nevertheless, the corresponding X-ray measurements with atomic hydrogen at solar wind velocities are sparse.

Here, the X-ray emissions are reported with a high resolution X-ray calorimeter detector for CX between O^{8+} and Kr. The O^{8+} projectile velocities are from 293 km/s to 1256 km/s, which is characteristic of the solar wind (SW) ions. The first ionization energy of Kr (14.0 eV) is close to that of hydrogen (13.6 eV), so the state selectivity during the single capture should be similar. On the other hand, multi-electron processes are possible, such as double capture, transfer ionization, triple capture, etc. Since transfer ionization cross sections fall off exponentially with decreasing collision energies, the X-ray spectra contribution from transfer ionization can be neglected here [22]. We note that, with aid of the Molecular Classical over-Barrier Model (MCBM) [23], the estimated cross sections for double capture even triple capture are roughly comparable to that of single capture for the present system. This indicates that multiple capture processes are most likely involved in creating some excited states whose stabilization contributes to soft X-ray emission.

II. EXPERIMENT

Charge exchange between O^{8+} and Kr was measured using a beam-gas cell technique at the Oak Ridge National Laboratory Multicharged Ion Research Facility. X-ray spectra were measured using a X-ray quantum microcalorimeter (XQC) from the University of Wisconsin and Goddard Space Flight Center [17, 24]. The sketch of the experimental setup can be seen in Fig. 1 and is identical to that used in other measurements [16–18].

Briefly, $^{18}O^{8+}$ ions were produced by an electron cyclotron resonance (ECR) ion source,

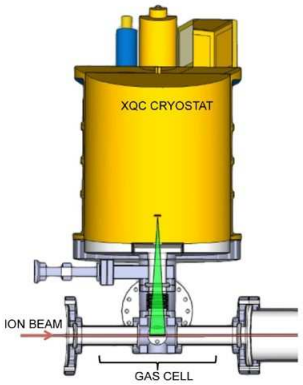

FIG. 1. (Color online) Schematic of the CX cell with the XQC and the O^{8+} beam passing through Kr gas. The viewable portion of the gas cell is shown as the solid angle from the detector array.

extracted at 17.7 kV, momentum analyzed by a 90° dipole magnet, and then accelerated or decelerated to the desired ion energies of 445 eV/u, 889 eV/u, 1780 eV/u, and 8180 eV/u. Several sets of einzel lenses and adjustable slits are installed in the beam line so as to focus and collimate the primary beam size to a few mm in diameter in the Kr gas cell. The XQC is a 6 × 6 pixel array of microcalorimeters with HgTe absorbers each 2.0 mm × 2.0 mm and 0.7 μm in thickness. The gas cell is 20 cm long. XQC was operated at 50 mK and positioned 23 cm above the beam, with a solid angle of 2.3 $\times 10^{-3}$ sr for measuring the prompt X-rays emitted at 90° with respect to the beam direction.

During the experiment, approximately 0.3 nA of O^{8+} ions were incident on krypton gas for beam energies of 445 eV/u, 889 eV/u, and 1780 eV/u and 4.0 nA for the beam energy of 8180 eV/u. Krypton was introduced into the gas cell via a leak valve and the total pressure was monitored by a nude Bayard-Alpert ion gauge and a quadrapole residual gas analyzer (SRS RGA 100). The pressure in the cell was adjusted and maintained so that the detector count rate was less than 1 Hz per pixel which limited pulse pileup. Measured gas pressures were in the range $\sim 2 \times 10^{-5}$ Pa. XQC was protected from thermal (IR) radiation by a set of thin aluminum filters which were periodically defrosted. The X-ray backgrounds from the ion beam (without gas) and dark counts were periodically measured and found to be insignificant.

When calculating line ratios, the measured line intensities were corrected for the energy-dependent efficiencies of the filters, which are 0.4997, 0.6057, 0.5334, 0.6453, and 0.6510 for Ly-α, Ly-β, Ly-γ, Ly-δ, and Ly-ε, respectively. Because the calculated polarizations are

small [25] for O^{8+} - H system and the error in cross sections due to anisotropy can never be larger than 30% even if the X-rays are fully polarized [10, 26], differences between the line ratios with the X-ray spectrum intensities detected at 90° and 54° (so-called magic angle) [27] are not expected to be significant.

III. CASCADE MODEL

For the one-electron capture process, the observed X-ray count rates are a function of both the angular momentum (n, l) distribution of the captured electrons and the effect of radiative cascades. Calculations of single charge exchange (SCX) for O^{8+} + H collisions indicate that capture occurs primarily to the $n = 5$ states of O^{7+} for energies above 1 keV/u [19, 20, 28]. At lower energies, there is some discrepancy among calculations for the relative dominance of $n = 5$, 6 channels, but the $n = 7$ and the $n = 4$ contributions to the total cross section is negligible (less than 5 % for energies less than 6 keV/u) and there is no capture to $n \leq 3$ [21, 28, 29]. Due to the similar ionization potential of Kr and H, the dominant capture channels are expected to be qualitatively similar for O^{8+} - Kr SCX, which is described as follows.

$$\begin{aligned} O^{8+} + Kr(4p^6\ {}^1S) &\rightarrow O^{7+}(n \sim 4-6) + Kr^+(4p^5\ {}^2P^o) \\ &\rightarrow O^{7+}(1s) + \gamma + Kr^+(4p^5\ {}^2P^o) \end{aligned} \tag{1}$$

Theoretical O^{8+} + H SCX line ratios were determined from the calculated state selective cross sections, $\sigma_{n,l}$, with n = 4, 5, and 6 along with branching ratios. Expressions for O^{7+} emission cross sections for Ly-α Ly-β, Ly-γ, Ly-δ, and Ly-ε are shown in Eqs. (2 - 6).

$$\begin{aligned} \sigma^{emiss}_{2p\rightarrow 1s} = {} & \sigma(6h) + 0.956\sigma(6g) + 0.863\sigma(6f) + 0.627\sigma(6d) \\ & + 0.038\sigma(6p) + 0.409\sigma(6s) + \sigma(5g) \\ & + 0.908\sigma(5f) + 0.664\sigma(5d) + 0.056\sigma(5p) \\ & + 0.454\sigma(5s) + \sigma(4d) + 0.746\sigma(4d) \\ & + 0.042\sigma(4p) + 0.585\sigma(4s) \end{aligned} \tag{2}$$

$$\begin{aligned}\sigma^{emiss}_{3p\rightarrow 1s} = & 0.038\sigma(6g) + 0.105\sigma(6f) + 0.198\sigma(6d) \\ & + 0.019\sigma(6p) + 0.240\sigma(6s) + 0.081\sigma(5f) \\ & + 0.208\sigma(5d) + 0.007\sigma(5p) + 0.281\sigma(5s) \\ & + 0.224\sigma(4d) + 0.366\sigma(4s)\end{aligned} \tag{3}$$

$$\begin{aligned}\sigma^{emiss}_{4p\rightarrow 1s} = & 0.015\sigma(6f) + 0.086\sigma(6d) + 0.008\sigma(6p) \\ & + 0.161\sigma(6s) + 0.087\sigma(5d) + 0.190\sigma(5s) \\ & + 0.839\sigma(4p)\end{aligned} \tag{4}$$

$$\sigma^{emiss}_{5p\rightarrow 1s} = 0.044\sigma(6d) + 0.117\sigma(6s) + 0.818\sigma(5p) \tag{5}$$

$$\sigma^{emiss}_{6p\rightarrow 1s} = 0.780\sigma(6p) \tag{6}$$

Branching ratios were determined from Einstein A-values for radiative transitions from n, l to n', l', $A_{nl\rightarrow n'l'}$, which were statistically averaged over total angular momentum j. The transit time, Δt, of ions across the field of view of the detector is in the range 16 ns - 68 ns ($1/\Delta t \sim 1.5$ - 6.3×10^7 s^{-1}). This is larger than the lifetimes of the populated excited states and covers all the possible transitions.

IV. AUTOIONIZING DOUBLE CAPTURE

The above model in Section III is for SCX with an atomic hydrogen target. When a multi-electron target is involved, autoionizing double even triple capture processes can occur. It has previously been observed that the relative cross sections of autoionizing double capture is larger than that of autoionozing triple capture with respect to that of single capture in 0.8 keV/u O^{8+} collisions with Kr [30, 31]. Several studies have investigated the autionizing double capture contribution for various collision systems, such as C^{6+} + H_2, O^{8+} + He, Ne^{10+} + H_2O, etc. [17, 32–34]. Chetiou *et al.* [35] have pointed out that doubly excited states can autoionize into lower singly excited states followed by Ly-α or Ly-β X-ray emission in 1.24 keV/u O^{8+} collisions with He and H_2. These processes are as follows.

$$\begin{aligned}O^{8+} + He(1s^2\ ^1S) & \rightarrow O^{6+}(3lnl\ n \sim 3-4) + He^{2+} \\ & \rightarrow O^{7+}(2p) + He^{2+} + e \\ & \rightarrow O^{7+}(1s) + \gamma + He^{2+} + e\end{aligned} \tag{7}$$

$$
\begin{aligned}
O^{8+} + H_2 &\rightarrow O^{6+}(4l4l') + H^+ + H^+ \\
&\rightarrow O^{7+}(3p) + H^+ + H^+ + e \\
&\rightarrow O^{7+}(1s) + \gamma + H^+ + H^+ + e
\end{aligned} \tag{8}
$$

Similar autoionizing double capture channels are expected for O^{8+} collisions with Kr.

V. RESULTS AND DISCUSSION

Figure $2(a) - (d)$ show the X-ray spectra measured in O^{8+} and Kr collisions for the incident velocities of 293 km/s, 414 km/s, 586 km/s, and 1256 km/s. Gaussian curve fitting was adopted to extract the contribution of the different transitions, as shown in Figure 2(e) for 293 km/s. Clearly, $2p \rightarrow 1s$, $3p \rightarrow 1s$, $4p \rightarrow 1s$, $5p \rightarrow 1s$, $6p \rightarrow 1s$ transitions, correspondingly labeled as Ly-α, Ly-β, Ly-γ, Ly-δ, and Ly-ε, are observed for the singly excited O^{7+} ion formed through SCX between O^{8+} and Kr. The spectra also show a prominent peak at about 570 eV which is probably a mixture of the resonant transition from singly excited state $1s2p(^1P_1)$ to ground state $1s^2(^1S_0)$ and the nearby intercombination transition in O^{6+} ion.

The full width at half maximum (FWHM) of the fitted peaks was constrained to be the same for each spectrum. Peak widths changed slightly between spectra (9.2 eV - 9.8 eV), as shown in Figure 2(e). Additional Gaussian functions with unconstrained FWHM were initially located at 640 eV, 743 eV, and 765 eV to minimize the reduced χ^2 value of the composite fitting in all spectra. The peaks are tentatively identified to be the doubly excited transitions $2p^2(^1S, {}^1D)$-$1s2p(^1P)$, $2s2p(^1P)$-$1s2s(^1S)$ and $2p3d(^1D)$-$1s2p(^1P)$, and $3p^2(^3P)$-$1s3p(^3P)$, respectively[36–38]. These peaks are from double-electron capture processes, and not included in our reported ratios here.

The experimentally determined line ratios of the Lyman series as a function of velocity are shown in Table I. The Ly-β/Ly-α ratio is the largest, in part because the Ly-β ($3p \rightarrow 1s$) transition is being fed by more cascades from higher lying states than Ly-γ, Ly-δ, or Ly-ε.

Figures 3-6 show the observed emission line ratios for O^{8+} + Kr and the constructed theoretical SCX line ratios for O^{8+} + H as a function of velocity. The constructed emission line ratios take all possible cascades into account (see Eqs. 2-6). In Figure 3, the measured

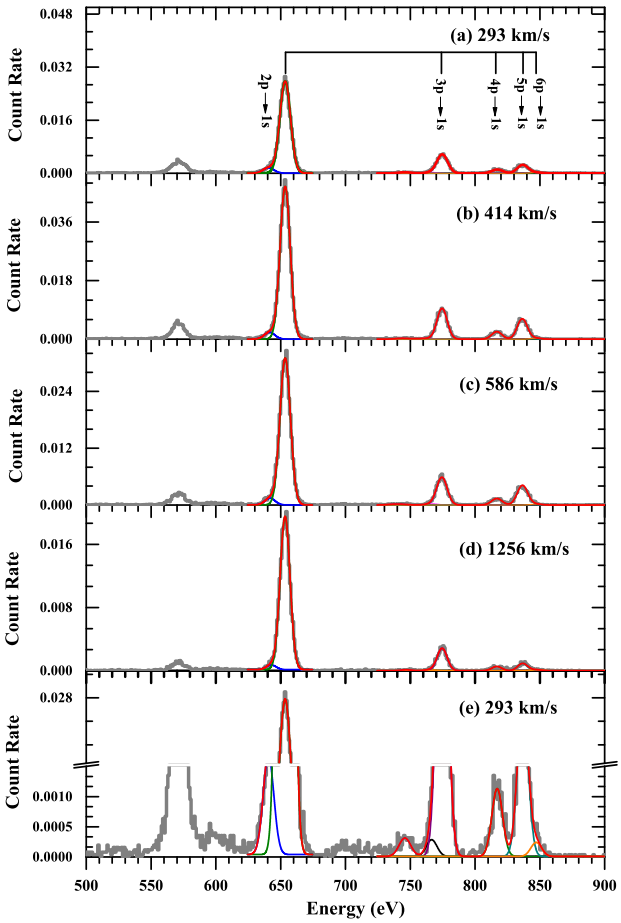

FIG. 2. (Color online) X-ray spectra for O^{8+} on Kr. Gray lines and color lines represent the experimental data and Gaussian fitting results, respectively. (a), (b), (c), (d) represent the incident projectile velocities of 293 km/s, 414 km/s, 586 km/s and 1256 km/s, respectively. (e) shows the Gaussian peak fitting at 293 km/s.

TABLE I. Experimentally determined line ratios for O^{8+} + Kr collisions. Errors are determined from the standard errors in the fitted areas of the peaks.

E (eV/u)	v (km/s)	Ly-β/Ly-α	Ly-γ/Ly-α	Ly-δ/Ly-α	Ly-ε/Ly-α
445	293	0.169 ± 0.044	0.032 ± 0.008	0.071 ± 0.014	0.0065 ± 0.0038
889	414	0.165 ± 0.030	0.039 ± 0.012	0.103 ± 0.020	0.0050 ± 0.0076
1780	586	0.154 ± 0.066	0.035 ± 0.008	0.104 ± 0.015	0.0048 ± 0.0061
8180	1256	0.121 ± 0.027	0.022 ± 0.004	0.037 ± 0.011	0.0048 ± 0.0028

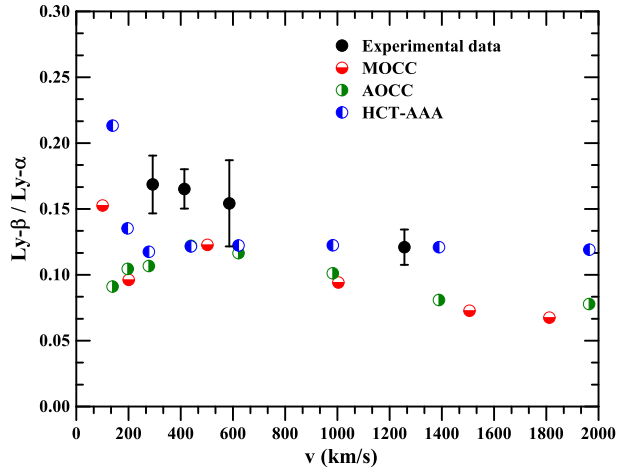

FIG. 3. (Color online) Ly-β/Ly-α line ratios for X-ray emission in O^{8+} + Kr collisions. The experimental data is represented by solid circles. Theoretical ratios are calculated from O^{8+} + H collision theories; Shipsey *et al.* (MOCC) [19], Fritsch *et al.* (AOCC) [20] and Richter *et al.* (HCT-AAA) [21]. See text for more details.

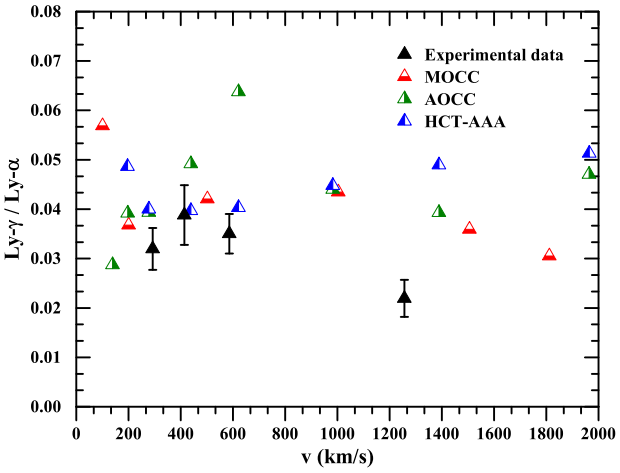

FIG. 4. (Color online) Ly-γ/Ly-α line ratios for X-ray emission in O^{8+} + Kr collisions. The experimental data is represented by solid triangles. Theoretical ratios are calculated from O^{8+} + H collision theory; Shipsey *et al.* (MOCC) [19], Fritsch *et al.* (AOCC) [20] and Richter *et al.* (HCT-AAA) [21]. See text for more details.

Ly-β/Ly-α ratios tend to be in agreement with the constructed ratios using the SCX calculation of Richter *et al.* (HCT-AAA) [21] at the projectile velocity of 1256 km/s, while the experimental line ratios are higher than theoretical ratios for the projectile velocity of 293, 414, and 586 km/s. This probably results from an autoionizing double capture (ADC) feed-

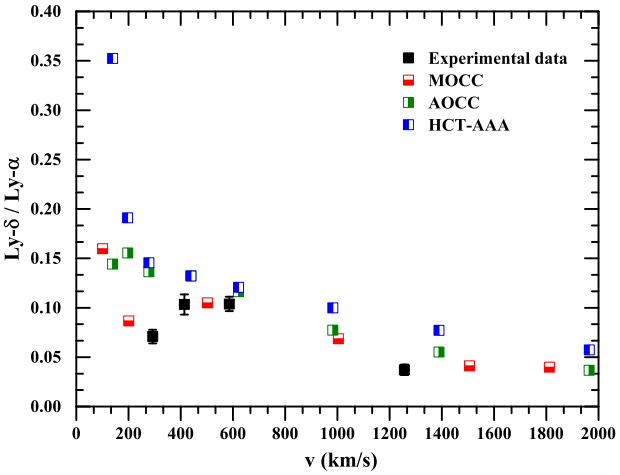

FIG. 5. (Color online) Ly-δ/Ly-α line ratios for X-ray emission in O^{8+} + Kr collisions. The experimental data is represented by solid squares. Theoretical ratios are calculated from O^{8+} + H collision theories; Shipsey *et al.* (MOCC) [19], Fritsch *et al.* (AOCC) [20] and Richter *et al.* (HCT-AAA) [21]. See text for more details.

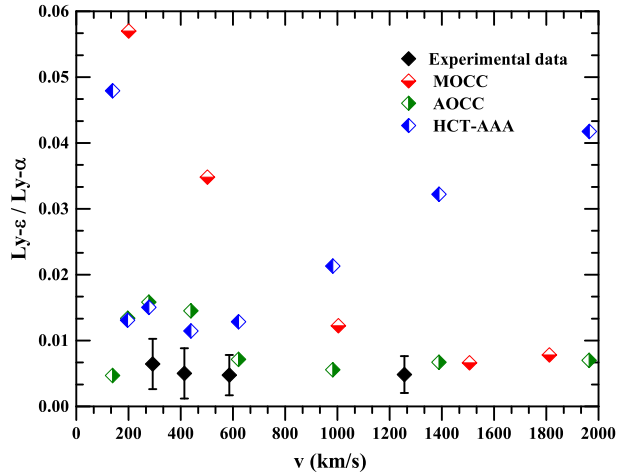

FIG. 6. (Color online) Ly-ε/Ly-α line ratios for X-ray emission in O^{8+} + Kr collisions. The experimental data is represented by solid diamonds. Theoretical ratios are calcuated from O^{8+} + H collision theories; Shipsey *et al.* (MOCC) [19], Fritsch *et al.* (AOCC) [20] and Richter *et al.* (HCT-AAA) [21]. See text for more details.

ing mechanism, as shown in Eq. 8, that is doubly excited states $4l4l$ formed through double capture first decay essentially to the $3p\epsilon l'$ ($\epsilon l'$ represents continuum states of autoionized electron) and then $3p$ decays into $1s$ by Ly-β emission.

In Figure 4, the measured Ly-γ/Ly-α line ratios show good agreement at low velocities

with the theoretical ratios constructed using the SCX calculation of HCT-AAA [21] and MOCC [19]. Capture to the n=4 states is strongly dependent on velocity [21] and is predicted to be negligible at low velocities. The observed Ly-γ transition is probably fed by cascade from higher states $5s$, $5d$, $6s$, $6d$, etc.. At the highest velocity, there is a discrepancy between the measured and theoretical ratios. Theoretical calculations for nondominant channels are difficult and in this case may have overestimated the Ly-γ emission. Theory and experimental Ly-δ/Ly-α line ratios are more consistent with each other in Figure 5, due to the dominance of $n = 5$ capture for the current system.

The largest difference between the experimental results and theoretical O^{8+} + H SCX line ratios is evident in Figure 6 for Ly-ε/Ly-α. While at the highest velocity the measured line ratio is in good agreement with the theoretical ratios using Fritsch and Shipsey *et al.*, at the the lower velocities it is clear that the measured Ly-ε/Ly-α ratios are consistently smaller than theory. Note that the intensity of Ly-ε is a direct measurement of electron capture into the $6p$ state and the SCX total cross section for $n = 6$ capture does not change drastically for the present projectile velocities [39]. Thus, the smaller measured line ratios strongly suggest that the intensity of Ly-α is enhanced by a factor of two which provides a clear indication of double capture and triple capture contributions. Specifically, ADC as shown in Eq. 7 is the exclusive decay path to feed $O^{7+}(2p)$ states and consequently will enhance Ly-α emission. Autoionizing triple capture is less important than ADC [30, 31].

VI. CONCLUSIONS

Lyman spectra and line-ratios for soft X-ray emission following charge exchange between O^{8+} and Kr were measured using a beam-gas technique and a high resolution microcalorimeter X-ray detector for the collision velocities 293, 414, 586, and 1256 km/s. Ly-α, Ly-β, Ly-γ, Ly-δ, Ly-ε lines of the O^{7+} ion were identified, as well as minor transition lines from O^{6+}. Our observed line ratios are compared to a SCX model, specifically with theoretical calculations for O^{8+} + H. Good agreement is found for the line ratio from the dominant $n = 5$ shell, with direct capture and cascade having an important influence on the line ratio from the $n = 4$ shell. Moreover, for velocities lower than 600 km/s, X-ray emission following ADC results in Ly-α and Ly-β enhancement; the former leads to the Ly-ε/Ly-α line ratio significantly smaller than the single charge transfer theory, and the latter leads to the Ly-

β/Ly-α line ratio larger than theory. The present studies indicate that the ADC feeding mechanism is important and should be taken into account for the X-ray emission during multi-charged ion multi-electron atom collisions. The present study serves as an important benchmark for resolving angular momentum quantum states and subsequent decay schemes for theory when both single and multiple electron capture are present. This is a challenge for other experimental measurements, even the well-developed cold target recoil ion momentum spectroscopy [40].

VII. ACKNOWLEDGMENTS

This research is supported in part by NASA Astrophysics Research and Analysis Grant No. NNH13ZDA001N and NASA Solar and Heliospheric Grant No. NNX13AF31G. V.A. is supported by the National Science Foundation through Grant No. PHY-1068877. DGS appreciates support from the Albion College Faculty Development Fund.

[1] D. Bodewits, D. J. Christian, M. Torney, M. Dryer, C. M. Lisse, K. Dennerl, T. H. Zurbuchen, S. J. Wolk, A. G. G. M. Tielens, and R. Hoekstra, A & A **469**, 1183 (2007).

[2] R. C. Isler, Plasma Phys. Control. Fusion **33**, 549 (1991).

[3] S. Otranto and R. E. Olson, J. Phys. B: At. Mol. Phys. **43**, 155203 (2010).

[4] C. M. Lisse, K. Dennerl, J. Englhauser, M. Harden, F. E. Marshall, M. J. Mumma, R. Petre, J. P. Pye, M. J. Ricketts, J. Schmitt, J. Trümper, and R. G. West, Science **274**, 205 (1996).

[5] V. Krasnopolsky, J. Greenwood, and P. Stancil, Space. Sci. Rev **113**, 271 (2004).

[6] T. E. Cravens, Astrophys. J. Lett **532**, L153 (2000).

[7] B. J. Wargelin, M. Markevitch, M. Juda, V. Kharchenko, R. Edgar, and A. Dalgarno, Astrophys. J. **607**, 596 (2004).

[8] S. L. Snowden, M. R. Collier, and K. D. Kuntz, Astrophys. J. **610**, 1182 (2004).

[9] D. Koutroumpa, R. Lallement, J. C. Raymond, and V. Kharchenko, Astrophys. J. Lett **696**, 1517 (2009).

[10] A. C. K. Leung and T. Kirchner, Phys. Rev. A **93**, 052710 (2016).

[11] B. H. Bransden and M. R. C. McDowell, *charge exchange and the theory of ion-atom collisions* (Oxford Unversity Press, 1992).

[12] W. Fritsch and C. Lin, Phys. Rep **202**, 1 (1991).

[13] J. L. Nolte, P. C. Stancil, H. P. Liebermann, R. J. Buenker, Y. Hui, and D. R. Schultz, J. Phys. B: At. Mol. Phys. **45**, 245202 (2012).

[14] H. Ryufuku, K. Sasaki, and T. Watanabe, Phys. Rev. A **21**, 745 (1980).

[15] J. Burgdorfer, R. Morgenstern, and A. Niehaus, J. Phys. B: At. Mol. Phys. **19**, L507 (1986).

[16] X. Defay, K. Morgan, D. McCammon, D. Wulf, V. M. Andrianarijaona, M. Fogle, D. G. Seely, I. N. Draganić, and C. C. Havener, Phys. Rev. A **88**, 052702 (2013).

[17] M. Fogle, D. Wulf, K. Morgan, D. McCammon, D. G. Seely, I. N. Draganić, and C. C. Havener, Phys. Rev. A **89**, 042705 (2014).

[18] V. M. Andrianarijaona, D. Wulf, D. McCammon, D. G. Seely, and C. C. Havener, Nucl. Instr. Meth. B: **345**, 69 (2015).

[19] E. J. Shipsey, T. A. Green, and J. C. Browne, Phys. Rev. A **27**, 821 (1983).

[20] W. Fritsch and C. D. Lin, Phys. Rev. A **29**, 3039 (1984).

[21] K. Richter and E. A. Solov'ev, Phys. Rev. A **48**, 432 (1993).

[22] V. A. Krasnopolsky, J. B. Greenwood, and P. C. Stancil, Space Sci. Rev. **113**, 271 (2004).

[23] A. Niehaus, J. Phys. B: At. Mol. Phys. **19**, 2925 (1986).

[24] D. McCammon, K. Barger, D. E. Brandl, R. P. Brekosky, S. G. Crowder, J. D. Gygax, R. L. Kelley, C. A. Kilbourne, M. A. Lindeman, F. S. Porter, L. E. Rocks, and A. E. Szymkowiak, J. Low Temp. Phys. **151**, 715 (2008).

[25] C. D. Lin and J. H. Macek, Phys. Rev. A **35**, 5005 (1987).

[26] D. Dijkkamp, Y. S. Gordeev, A. Brazuk, A. G. Drentje, and F. J. de Heer, J. Phys. B: At. Mol. Phys. **18**, 737 (1985).

[27] B. L. Moiseiwitsch and S. J. Smith, Rev. Mod. Phys. **40**, 238 (1968).

[28] T.-G. Lee, M. Hesse, A.-T. Le, and C. D. Lin, Phys. Rev. A **70**, 012702 (2004).

[29] E. Edgu-Fry, A. Wech, J. Stuhlman, T. G. Lee, C. D. Lin, and C. L. Cocke, Phys. Rev. A **69**, 052714 (2004).

[30] S. Martin, J. Bernard, L. Chen, A. Denis, and J. Dèsesquelles, Phys. Rev. Lett **77**, 4306 (1996).

[31] S. Martin, J. Bernard, A. Denis, J. Dèsesquelles, L. Chen, and Y. Ouerdane, Phys. Rev. A **50**, 2322 (1994).

[32] F. W. Meyer, A. M. Howald, C. C. Havener, and R. A. Phaneuf, Phys. Rev. A **32**, 3310 (1985).

[33] S. Otranto and R. E. Olson, Phys. Rev. A **77**, 022709 (2008).

[34] R. Hoekstra, A. R. Schlatmann, F. J. de. Heer, and R. Morgenstern, J. Phys. B: At. Mol. Phys. **22**, L603 (1989).

[35] A. Chetioui, F. Martín, M. F. Politis, J. P. Rozet, A. Touati, L. Blumenfeld, D. Vernhet, K. Wohrer, C. Stephan, M. Barat, M. N. Gaboriaud, H. Laurent, and P. Roncin, J. Phys. B: At. Mol. Opt. Phys. **23**, 3659 (1990).

[36] D. L. Matthews, W. J. Braithwaite, H. H. Wolter, and C. F. Moore, Phys. Rev. A **8**, 1397 (1973).

[37] K. Dere, E. Landi, H. Mason, B. M. Fossi, and P. Young, Astron. Astrophys. Suppl. Ser. **125**, 149 (1997).

[38] D. Zanna, D. G, Y. K. P, P. R. Landi, E. Mason, and H. E, Astron. Astrophys. **582**, A56 (2015).

[39] L. Liu, J. G. Wang, and R. K. Janev, Phys. Rev. A **79**, 052702 (2009).

[40] J. Ullrich, R. Moshammer, A. Dorn, R. Dörner, L. P. H. Schmidt, and H. Schmidt-Böcking, Rep. Prog. Phys. **66**, 1463 (2003).